ROYAL SOCIETY
OF CHEMISTRY

PAPER

Check for updates

Benzothiazole-based arylamines as hole transporting materials for perovskite solar cells†

Povilas Luizys,‡[a] Shun Tian,‡[b] Kasparas Rakstys, [ID] *[a] Roland C. Turnell-Ritson,[c] Valdas Paulauskas, [ID] [d] Vygintas Jankauskas,[e] Vytautas Getautis [ID] [a] and Mohammad Khaja Nazeeruddin [ID] *[bf]

The performance of perovskite solar cells (PSCs) is partially dependent on the properties of the hole transporting material (HTM) used. Here, we present the synthesis and study of novel benzothiazole-based arylamine HTMs. The compounds are thermally stable, decomposing at temperatures >350 °C, and exist in amorphous states. The ionization potential values of the HTMs are between 5.26–5.62 eV, which are optimal with respect to the valence band energy of perovskite (~5.7 eV). PSCs employing the best performing HTM resulted in a power conversion efficiency (PCE) of 20.74% with a fill factor (FF) of 77.6%. With this we present donor–π–bridge–acceptor type-strategy as an effective method to increase charge transport properties of benzothiazole-based small molecule HTMs that are obtained in high yield *via* a simple Knoevenagel condensation reaction resulting in improved performance of the hole transporting layer in PSCs.

Introduction

Over the past several years, fast development of hybrid organic–inorganic perovskite solar cells (PSCs) has made them one of the major research subjects in the field of photovoltaics as alternatives to current silicon-based solar cells.[1] During 2009, the first PSC devices were demonstrated by Kojima and co-workers,[2] with a power conversion efficiency (PCE) of 3.1%. Since then, the performance of PSCs has increased significantly, to a current record of 26.7% for single junction devices.[3] PSCs exhibit impressive photovoltaic performance due to the excellent optoelectronic properties of perovskite materials.[4–9]

In general, the structure of a PSC device consists of a multi-layered stack, where the light-absorbing perovskite layer is positioned between an electron transporting material (ETM) layer and hole transporting material (HTM) layer.[10] The charge transporting layers facilitate more effective charge extraction/collection and prevent charge recombination, which is essential for producing high efficiency solar cells.[11] Typically, titanium dioxide (TiO₂) is used as the ETM, while the most commonly used HTM in PSCs is 2,2′,7,7′-tetrakis(N,N-di-p-methoxyphenylamine)-9,9′-spirobifluorene (Spiro-OMeTAD). However, due to both the stability issues of Spiro-OMeTAD devices, which limits their lifetime, and a multi-step synthesis route, which results in a relatively high material cost, the search for stable and low-cost alternatives remains highly relevant to further PSC development.[12,13]

Substantial effort from many research groups has been directed towards the improved synthesis of small molecule HTMs which can reduce the cost and improve the stability of photovoltaic devices. Reported examples of novel HTMs include those based on fluorene-,[14,15] amide-,[16] enamine-,[17–19] carbazole-,[20–23] triphenylamine-,[24] pyrene-,[25,26] and thiophene-based[27–31] derivatives. One of the possible strategies for developing novel HTMs is to construct molecules consisting of an electron-donating unit (D) and electron-accepting units (A) as alternating electronic structures. The donor–acceptor type of molecules has been extensively investigated and widely adopted in the organic photovoltaic (OPV) field.[32] However, for application in PSCs, they have been rarely reported. Nevertheless, Liu and co-workers have developed a D–A type conjugated small molecule DOR3T-TBDT as a dopant-free HTM.[33] Due to its high hole mobility and conductivity, the photovoltaic cell constructed using a layer of DOR3T-TBDT reached a PCE of 14.9%, which was higher than the device fabricated using a

[a] *Department of Organic Chemistry, Kaunas University of Technology, Radvilenu pl. 19, Kaunas 50254, Lithuania. E-mail: kasparas.rakstys@ktu.lt*

[b] *Institute of Chemical Sciences and Engineering, École Polytechnique Fédérale de Lausanne (EPFL), Lausanne, 1015, Switzerland*

[c] *Department of Chemistry, Chemistry Research Laboratory, Mansfield Road, Oxford, OX1 3TA, UK*

[d] *Department of Environment and Ecology, Faculty of Forest Sciences and Ecology, Agriculture Academy, Vytautas Magnus University, Donelaicio St. 58, Kaunas 44248, Lithuania*

[e] *Institute of Chemical Physics Vilnius University, Sauletekio al. 3, Vilnius 10257, Lithuania*

[f] *Mechanical and Energy Engineering Department, College of Engineering, Imam Abdulrahman Bin Faisal University, Dammam, 34212, Saudi Arabia. E-mail: mdkhaja.nazeeruddin@epfl.ch*

† Electronic supplementary information (ESI) available. See DOI: https://doi.org/10.1039/d5tc01318f

‡ P. L. and S. T. contributed equally to this work.

layer of doped Spiro-OMeTAD (14.0%). Another useful strategy for designing novel organic semiconductors is to develop molecules of the type A–D–A, as reported by Steck and co-workers. In this example, two S,N-heteropentacene conjugated molecules were prepared, having suitable energy levels with respect to the MAPbI$_3$ perovskite. The resulting PSC devices gave favourable fill factor (FF) and open circuit voltage (V_{OC}) values, and PCEs of 10.3–11.4% without the use of additives.[34]

Potentially more interesting are HTM molecules of the type D–A–D. This molecular construction tends to have a low bandgap with a low-lying HOMO level, leading to an improvement in V_{OC}.[35] One example of this could be the work of Pham and co-workers, using triphenylamine (TPA) as the donor blocks and biphenyl fumaronitrile (BPFN) as the acceptor to synthesize new organic semiconductors of the type TPA–BPFN–TPA.[36] Devices using this new compound as a dopant-free HTM in PSCs achieved a V_{OC} value was 1.04 V with a PCE of 18.4%, while the doped Spiro-OMeTAD reached 1.00 V and 16.5%, respectively.

As can be seen from previously reported works, the use of donor and acceptor building blocks to fabricate new charge transportation materials has significant potential. By employing a donor–acceptor based molecular architecture approach, an alternative method is created to successfully prepare highly efficient HTMs, which should exhibit properties such as high charge carrier mobility and charge separation due to strong dipolar intermolecular interactions, suitable energy levels and improved stability and efficiency of the photovoltaic device.

Considering the promising properties of donor–acceptor type molecules, we designed and synthesized donor–π-bridge–acceptor A($-\pi$–D)$_n$ type small molecule HTMs systems and present them herein. To the best of our knowledge, benzothiazole-based derivatives bearing photoconductive triphenylamine chromophores linked by an aliphatic π-bridge have not been used as HTMs in PSCs. The optimized PSCs using the highest performing HTM, designated **V1671**, reached a PCE of 20.74%.

Results and discussions

The target HTMs **V1670**, **V1671** and **V1672** were obtained *via* Knoevenagel condensation of the respective benzo[n]thiazole derivatives with n equivalents of 4-[bis(4-methoxyphenyl)amino]-benzaldehyde in the presence of sodium hydride (Fig. 1). This results in a benzo[n]thiazole core connected through an ethenyl unit to a substituted triphenylamine chromophore. While the cores for $n = 1$ and $n = 2$ (2-methylbenzothiazole and 2,6-dimethylbenzo[1,2-d:4,5-d']bisthiazole, respectively) are commercially available, the core for $n = 3$ was prepared by a modification of literature methods.[37] The chemical structures of the HTMs were confirmed by ^{1}H NMR, ^{13}C NMR, mass spectrometry and elemental analysis (see ESI†).

The thermal stability of the prepared HTMs was examined by thermogravimetric analysis (TGA) and differential scanning calorimetry (DSC). The TGA results are provided in Fig. 2a, and the summarized properties are listed in Table 1. The TGA results show that the decomposition temperatures (T_{dec}) range between 362 °C and 443 °C, which is somewhat lower than that of Spiro-OMeTAD (T_{dec} = 449 °C).[38] The increase in T_{dec} values has been observed in the set of the synthesized HTMs, where the lowest 5% weight loss T_{dec} value of 362 °C has been reported for **V1670** containing one substituted triphenylamine chromophore, nevertheless, it is still reasonably high to indicate sufficient thermal stability required for PSCs.
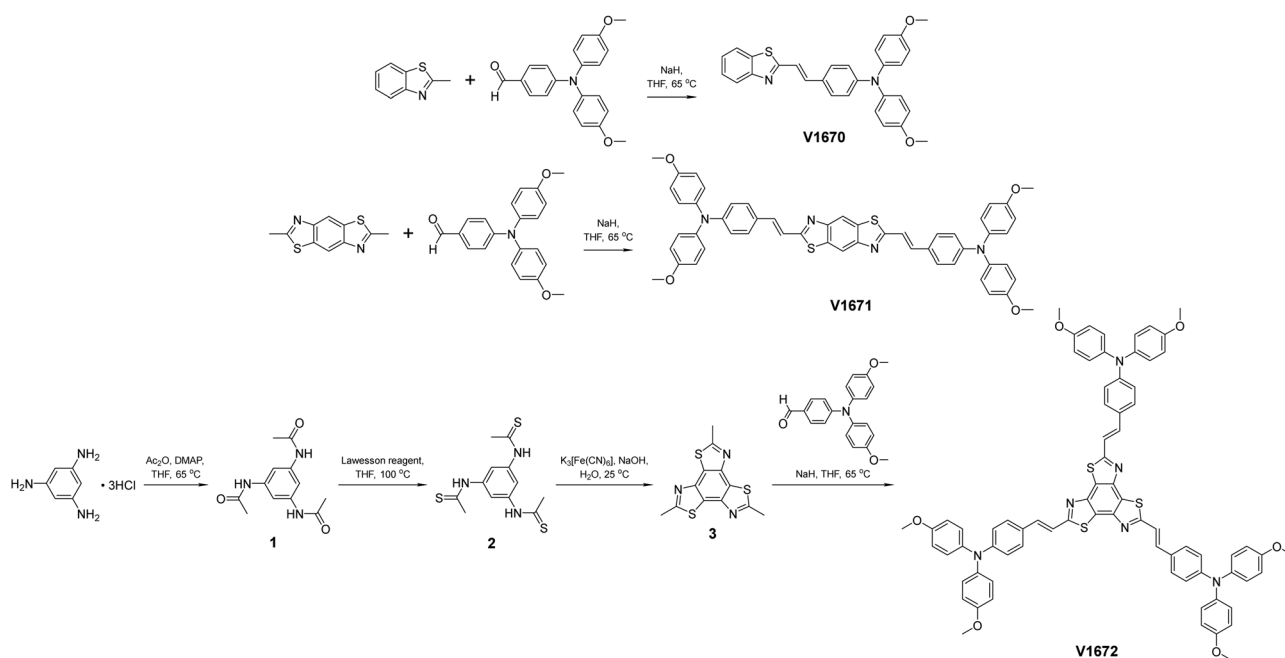

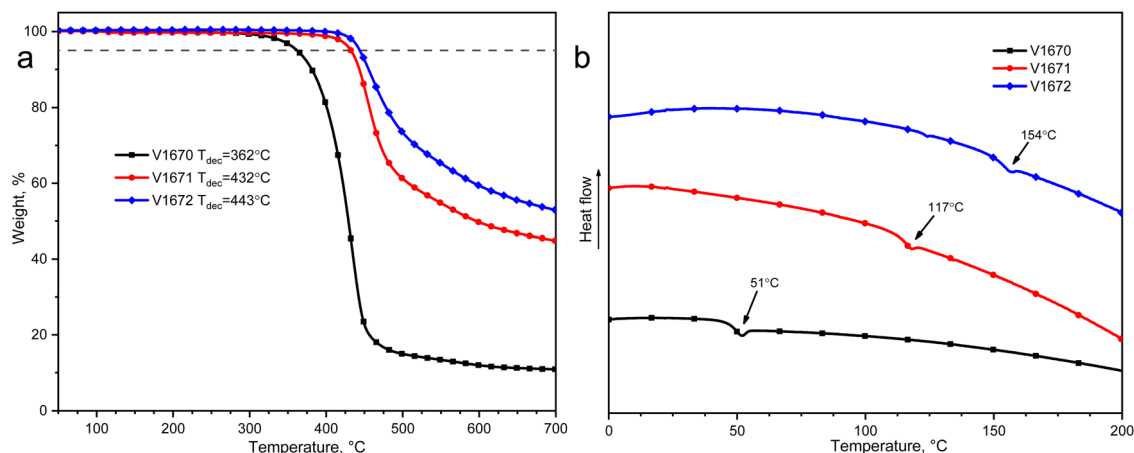Fig. 1 Synthesis of target compounds **V1670**, **V1671**, and **V1672**.

This journal is © The Royal Society of Chemistry 2025

J. Mater. Chem. C, 2025, **13**, 13502–13508 | **13503**

Fig. 2 (a) TGA heating curves of the target HTMs. (b) DSC curves of the second heating run.

Table 1 Thermal and photophysical properties of the HTMs

ID	$T_g{}^a$ (°C)	$T_{dec}{}^a$ (°C)	$\lambda_{PL}{}^b$ (nm)	$I_P{}^c$ (eV)	$E_g{}^d$ (eV)	$E_{ea}{}^e$ (eV)	$\mu_0{}^f$ (cm^2 V^{-1} s^{-1})	$\mu_0{}^g$ (cm^2 V^{-1} s^{-1})
V1670	51	362	572	5.26	2.46	2.80	2.6×10^{-6}	3.0×10^{-7}
V1671	117	432	593	5.62	2.23	3.39	2.7×10^{-6}	1.4×10^{-7}
V1672	154	443	588	5.57	2.29	3.28	–	3.6×10^{-7}

[a] Glass transition (T_g) and decomposition (T_{dec}) temperatures determined from DSC and TGA, respectively (10 °C min^{-1}, N$_2$ atmosphere). [b] UV-vis and PL spectra were measured in CB and CH$_2$Cl$_2$ (1:1 in volume) solutions (3.3 mM). [c] Ionization energies of the films measured using PESA. [d] E_g estimated optical bandgaps of HTMs. [e] $E_{ea} = I_P - E_g$. [f] Mobility value at zero field strength. [g] Drift carrier mobility measured with bisphenol-Z polycarbonate (PC-Z) (1:1).

Whereas highest recorded T_{dec} value are for **V1672** (443 °C) bearing three substituted triphenylamine chromophores. This tendency potentially can be explained by the higher molecular mass resulting in stronger intermolecular interactions.

DSC analysis shows that investigated HTMs **V1671** and **V1672** exist in an amorphous state since no endothermic melting peaks were observed over two heating cycles (Fig. S7, ESI†). However, for the compound **V1670** a melting temperature (T_m) was detected during the first heating cycle at 56 °C

and glass transition temperature (T_g) was measured during the second heating at 51 °C. Meanwhile for compounds **V1671** and **V1672** second heating scans showed glass transition at 117 °C and 154 °C, respectively. Furthermore, the data presented in Fig. 2b and Table 1 show that the T_g values increase significantly with an increasing number of substituted triphenylamine moieties, leading to a more stabilized amorphous state, which is generally desired for the formation of stable HTM films in PSCs.[38]
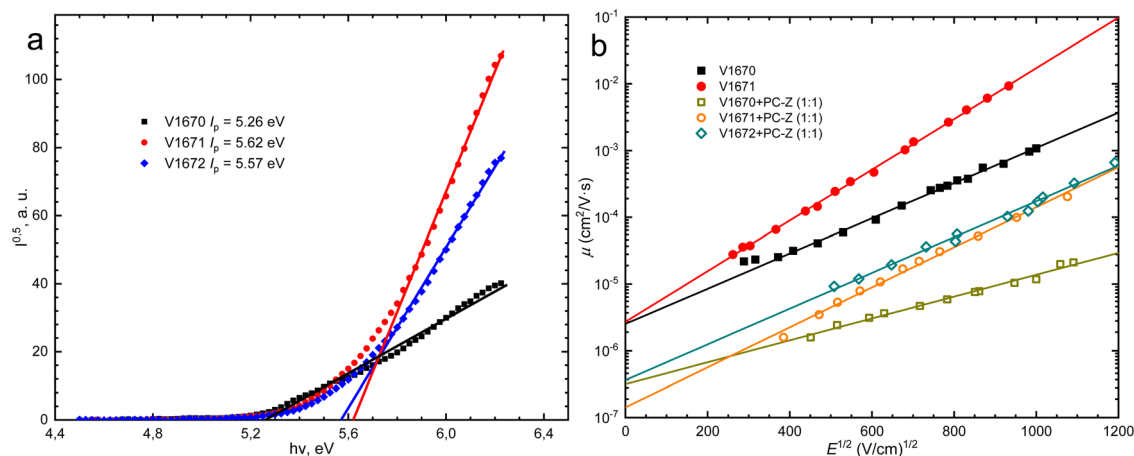

Fig. 3 (a) Photoemission in air spectra of **V1670**, **V1671** and **V1672**. (b) Electric field dependencies of the hole-drift mobility (μ) in the synthesized compounds, with and without PC-Z.

To better understand the energy level alignment of the target compounds in PSCs, we measured the solid-state ionization potential (I_p). I_p values of the novel HTMs were determined by the photoelectron emission spectroscopy in air (PESA) measurement of their thin films and give a reliable estimation of the highest occupied molecular orbital (HOMO) energy level. The recorded data is shown in Fig. 3a and Table 1. As seen from the measurement results, I_p values of **V1670**, **V1671** and **V1672** were found to be 5.26, 5.62, and 5.57 eV, respectively. The I_p values of HTMs are sufficiently close to optimally match with the valence band energy of perovskite ($\sim$5.7 eV), suggesting that the synthesized compounds would be suitable for use in PSCs.

The defining property of HTMs is their ability to selectively and efficiently transport holes. To investigate charge transport properties of the benzothiazole derivatives, hole drift mobilities were measured using the xerographic time of flight (XTOF) technique. The measurement results are presented in Fig. 3b and Table 1. Charge mobility values at zero-field strength (0 V cm^{-1}) are most significant, as electric fields are relatively weak in PSCs. Although the measured charge mobility of pure compounds **V1670** and **V1671** was 2.6×10^{-6} and 2.7×10^{-6} cm^2 V^{-1} s^{-1}, respectively, which is not particularly exceptional, it is sufficient for their application in PSCs. It should be noted that the quality of pure **V1672** layers was insufficient for XTOF measurements. To assess the hole drift mobility of **V1672**, it was mixed with a polycarbonate (PC-Z), and a film prepared. Addition of the polymer dilutes the HTM, reducing the overall charge mobility by roughly one order of magnitude;
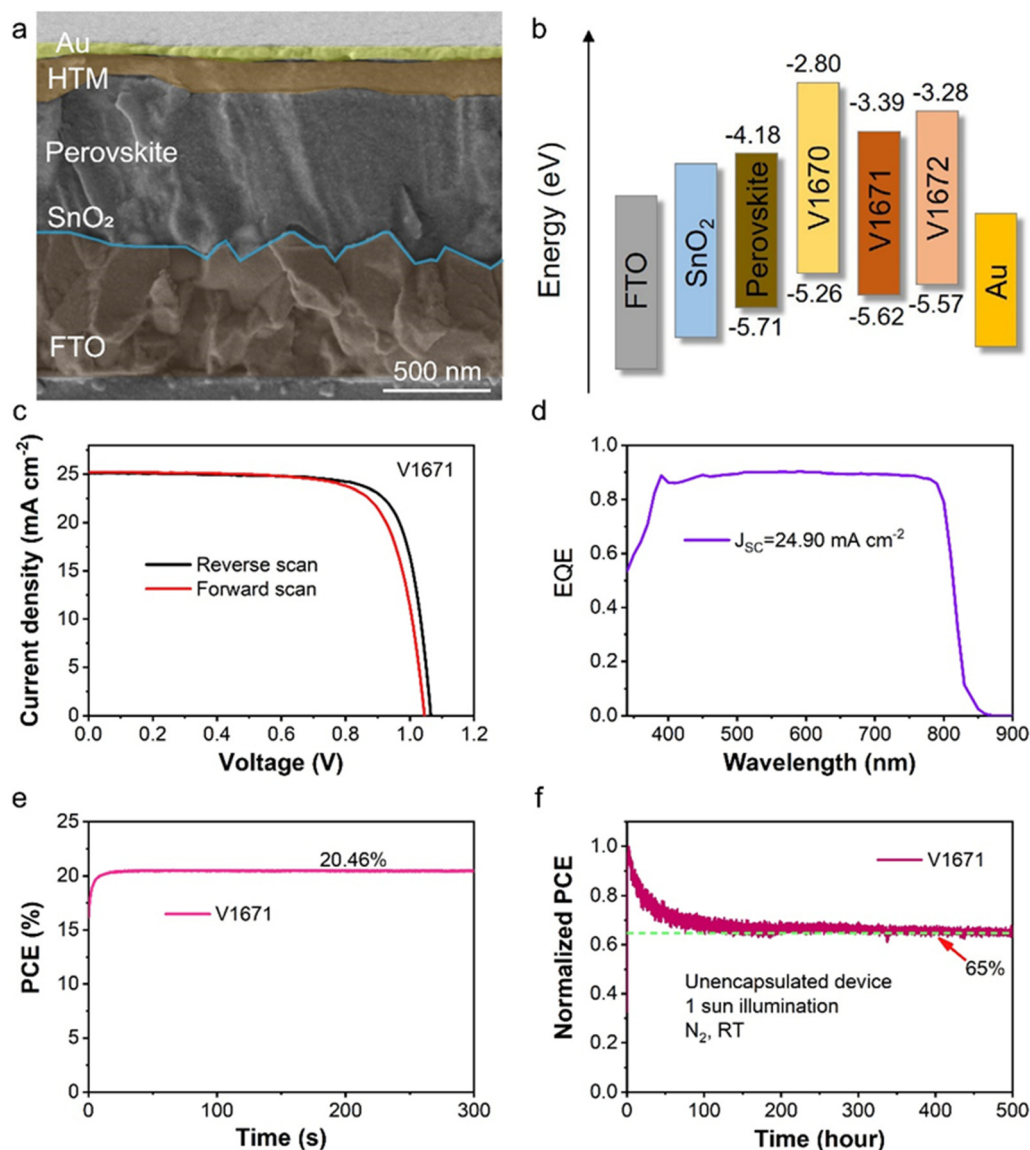

Fig. 4 (a) The cross-sectional SEM image of the n–i–p PSC structure. (b) The energy level diagram of each layer in the PSC. (c) Current density–voltage (*J*–*V*) curves of the PSC based on the **V1671** HTM under reverse and forward scan modes. (d) External quantum efficiency (EQE) spectra and the integrated J_{SC} of the corresponding PSC. (e) Steady power output of the champion target device for 300 s. (f) MPP tracking of the unencapsulated **V1671** PSC under continuous 1 Sun illumination in a N$_2$ atmosphere at room temperature.

This journal is © The Royal Society of Chemistry 2025

J. Mater. Chem. C, 2025, **13**, 13502–13508 | **13505**

however, it allowed for the measurement of **V1672** and its comparison with the other compounds. The XTOF measurement results of the HTMs with PC-Z shows that all three materials produce similar results under the same (diluted) conditions.

The PSC structure for the FTO/SnO$_2$/Perovskite/PEAI/HTM/Au was characterized by cross-section scanning electron microscopy (SEM) (Fig. 4a). The SnO$_2$ electron transport layers were fabricated by a chemical bath deposition (CBD) method according to a previous report.[39] The energy level diagram of each component in the PSCs is illustrated in Fig. 4b. As reported above, the HOMO energy level of **V1670**, **V1671** and **V1672** are −5.26, −5.62 and −5.57 eV and the optical bandgaps are 2.46, 2.23 and 2.29 eV, respectively (Fig. S8 and S9, ESI†). Therefore, the lowest unoccupied molecular orbitals (LUMOs) of the **V1670**, **V1671** and **V1672** are calculated to be −2.80, −3.39 and −3.28 eV, respectively. The valence band maximum (VBM) and conduction band minimum (CBM) of the perovskite film are −5.71 and −4.18 eV, respectively, which were determined by ultraviolet photoelectron spectroscopy (UPS) (Fig. S10, ESI†). The HOMO level of **V1671** has the lowest energy barrier relative to the VBM of the perovskite film among the three HTMs, indicating that photogenerated holes could be extracted efficiently from perovskite layer to the **V1671** HTM. The PSC based on this material shows the highest PCE with the enhancement of open-circuit voltage (V_{OC}) and short-circuit current density (J_{SC}) among the three HTMs (Fig. S11, ESI†), which could be attributed to its efficient charge extraction property and high hole drift mobility (Table 1).

The surface morphologies of the **V1670**, **V1671** and **V1672** films were measured by SEM, as shown in Fig. S12 (ESI†). The surface morphology of the **V1670** is highly homogeneous, whereas the **V1671** film is slightly less homogeneous and not pinhole-free. However, the **V1672** film has poor morphology, with many visible pinholes and a tendency to aggregate when spin-coating, which may affect the quality of HTM film and impede the PSC performance. Fig. S15 (ESI†) shows the TRPL spectra of perovskite and deposited HTLs. The effective lifetimes (defined as the time required for the PL intensity to decay to $1/e$ of its initial value after excitation) were 86.8, 1.8, 2.2, and 2.9 ns for the perovskite, perovskite/**V1670**, perovskite/**V1671**, and perovskite/**V1672** films, respectively. Compared to the pristine perovskite film, the perovskite/HTM films exhibit much shorter PL lifetimes, indicating efficient carrier extraction at the perovskite/HTM interface. Among the three HTMs, **V1671** shows the most efficient carrier extraction, consistent with its minimal energy barrier between its HOMO level and the VBM of the perovskite.

Further, the performance of the PSC based on **V1671** was optimized by adjusting its solution concentration during spin-coating (Fig. S13, ESI†) and the average photovoltaic parameters are summarized in Table S1 (ESI†). The PSCs based on 25 mg mL^{-1} **V1671** have the best surface morphology, and, correspondingly, the highest photovoltaic performance (Fig. S12b and S14, ESI†). A **V1671** concentration above 30 mg mL^{-1} led to significant reductions in J_{SC} and fill factor (FF) of the PSCs due to reduced homogeneity of the surface.

Table 2 Detailed photovoltaic parameters of the champion **V1671** device

V1671	V_{SC} (V)	J_{SC} (mA cm^{-2})	FF (%)	PCE (%)
Reverse	1.066	25.10	77.6	20.74
Forward	1.046	25.21	74.5	19.62

The champion **V1671** device had a V_{OC} of 1.066 V, a J_{SC} of 25.10 mA cm^{-2} and an FF of 77.6%, which resulted in a PCE of 20.74% at reverse scan (RS) (Fig. 4c). Its PCE at forward scan (FS) reached 19.62%. Detailed photovoltaic parameters are summarized in Table 2. The hysteresis index (HI) of the **V1671** device was 5.4%, as calculated using HI = (PCE$_{RS}$ − PCE$_{FS}$)/PCE$_{RS}$.[34] Compared to the **V1671** device, the Spiro-OMeTAD device shows a higher PCE of 21.8% with a smaller HI of 3.2% (Fig. S16, ESI†), indicating there is still a gap of molecular design. Fig. 4d shows the spectral dependence of the external quantum efficiency (EQE) for the **V1671** device. The integrated current density is 24.90 mA cm^{-2}, which is consistent with the J_{SC} value in Fig. 4c. Furthermore, the maximum power point tracking (MPPT) PCE of the device is 20.46%, stable over a 300 s measurement (Fig. 4e). In addition, the operational stability of the unencapsulated **V1671** device was evaluated at the MPP under a nitrogen atmosphere using a light-emitting diode lamp with a calibrated light intensity of 100 mW cm^{-2}. After 500 hours of measurement, the **V1671** device retained about 65% of its initial PCE (Fig. 4f). Water contact angle measurements revealed that all HTMs show higher contact angle comparing with bare perovskite films as shown in Fig. S17 (ESI†). **V1671** film exhibited a highest angle (83°) among the series, which is also higher than that of the spiro-OMeTAD (68°).[40] The greater hydrophobicity of **V1671** could be one of the reasons of high stability of the device that contains this HTM.

Conclusions

In conclusion, we report the synthesis and systematic study of the novel A(−π−D)$_n$ type small molecule HTMs for PSCs. The investigated benzothiazole-based arylamines were obtained in high yield *via* a simple Knoevenagel condensation reaction. The influence of the different number of triphenylamine chromophores has been evaluated by the thermal, optical, photophysical and photovoltaic measurements. It was found that as the number of triphenylamine fragments increases the decomposition and glass transition temperatures of the HTMs increase, and investigated compounds exist in an amorphous state which is desired in the fabrication of PSCs. Notably, the I_p values of HTMs are in the range of 5.26–5.62 eV, which is suitable for application in PSCs. Additionally, PSCs fabricated with **V1671** as the HTM resulted in the photovoltaic device achieving a PCE of 20.74% that is much higher than PCEs of **V1670** and **V1672** devices, which could be attributed to its higher hole drift mobility, better energy level alignment relative to the perovskite layer, and pinhole-free surface morphology. This work shows that the synthesis of new small molecule HTMs *via* a donor−π−

13506 | *J. Mater. Chem. C*, 2025, **13**, 13502–13508

This journal is © The Royal Society of Chemistry 2025

bridge–acceptor type-strategy is an effective method to improve the performance of the hole transporting layer in PSCs.

Data availability

The data that supports the findings of this study are available within the article and its ESI.† Additional data will be available online under repository link once the article will be accepted for publication, or from the corresponding author upon request. We note that there are not any restrictions on data availability (*e.g.*, proprietary data, privacy concerns).

Conflicts of interest

There are no conflicts to declare.

Acknowledgements

References

1 G. Hodes, *Science*, 1979, **2013**(342), 317–318.

2 A. Kojima, K. Teshima, Y. Shirai and T. Miyasaka, *J. Am. Chem. Soc.*, 2009, **131**, 6050–6051.

3 NREL, Best Research-Cell Efficiency Chart, **https://www.nrel.gov/pv/assets/pdfs/best-research-cell-efficiencies.pdf**, (accessed 3 February 2025).

4 Y. Rong, Y. Hu, A. Mei, H. Tan, M. I. Saidaminov, S. Il Seok, M. D. McGehee, E. H. Sargent and H. Han, *Science*, 2018, **361**, eaat8235.

5 W. Nie, H. Tsai, R. Asadpour, J.-C. Blancon, A. J. Neukirch, G. Gupta, J. J. Crochet, M. Chhowalla, S. Tretiak, M. A. Alam, H.-L. Wang and A. D. Mohite, *Science*, 2015, **347**, 522–525.

6 S. Park, J. H. Heo, C. H. Cheon, H. Kim, S. H. Im and H. J. Son, *J. Mater. Chem. A*, 2015, **3**, 24215–24220.

7 S. Kazim, M. K. Nazeeruddin, M. Grätzel and S. Ahmad, *Angew. Chem., Int. Ed.*, 2014, **53**, 2812–2824.

8 N.-G. Park, *J. Phys. Chem. Lett.*, 2013, **4**, 2423–2429.

9 R. Sharma, A. Sharma, S. Agarwal and M. S. Dhaka, *Sol. Energy*, 2022, **244**, 516–535.

10 A. S. R. Bati, Y. L. Zhong, P. L. Burn, M. K. Nazeeruddin, P. E. Shaw and M. Batmunkh, *Commun. Mater.*, 2023, **4**, 2.

11 M. Afroz, R. K. Ratnesh, S. Srivastava and J. Singh, *Sol. Energy*, 2025, **287**, 113205.

12 A. Jegorovè, M. A. Truong, R. Murdey, M. Daskeviciene, T. Malinauskas, K. Kantminiene, V. Jankauskas, V. Getautis and A. Wakamiya, *Solar RRL*, 2022, **6**, 2100877.

13 E. Kasparavicius, M. Franckevičius, V. Malinauskiene, K. Genevičius, V. Getautis and T. Malinauskas, *ACS Appl. Energy Mater.*, 2021, **4**, 13696–13705.

14 T. Malinauskas, M. Saliba, T. Matsui, M. Daskeviciene, S. Urnikaite, P. Gratia, R. Send, H. Wonneberger, I. Bruder, M. Graetzel, V. Getautis and M. K. Nazeeruddin, *Energy Environ. Sci.*, 2016, **9**, 1681–1686.

15 R. Tiazkis, S. Paek, M. Daskeviciene, T. Malinauskas, M. Saliba, J. Nekrasovas, V. Jankauskas, S. Ahmad, V. Getautis and M. Khaja Nazeeruddin, *Sci. Rep.*, 2017, **7**, 150.

16 M. L. Petrus, K. Schutt, M. T. Sirtl, E. M. Hutter, A. C. Closs, J. M. Ball, J. C. Bijleveld, A. Petrozza, T. Bein, T. J. Dingemans, T. J. Savenije, H. Snaith and P. Docampo, *Adv. Energy Mater.*, 2018, **8**, 1801605.

17 D. Vaitukaityte, Z. Wang, T. Malinauskas, A. Magomedov, G. Bubniene, V. Jankauskas, V. Getautis and H. J. Snaith, *Adv. Mater.*, 2018, **30**, 1803735.

18 M. Daskeviciene, S. Paek, Z. Wang, T. Malinauskas, G. Jokubauskaite, K. Rakstys, K. T. Cho, A. Magomedov, V. Jankauskas, S. Ahmad, H. J. Snaith, V. Getautis and M. K. Nazeeruddin, *Nano Energy*, 2017, **32**, 551–557.

19 M. Daskeviciene, S. Paek, A. Magomedov, K. T. Cho, M. Saliba, A. Kizeleviciute, T. Malinauskas, A. Gruodis, V. Jankauskas, E. Kamarauskas, M. K. Nazeeruddin and V. Getautis, *J. Mater. Chem. C*, 2019, **7**, 2717–2724.

20 C. Lu, I. T. Choi, J. Kim and H. K. Kim, *J. Mater. Chem. A*, 2017, **5**, 20263–20276.

21 A. Magomedov, S. Paek, P. Gratia, E. Kasparavicius, M. Daskeviciene, E. Kamarauskas, A. Gruodis, V. Jankauskas, K. Kantminiene, K. T. Cho, K. Rakstys, T. Malinauskas, V. Getautis and M. K. Nazeeruddin, *Adv. Funct. Mater.*, 2018, **28**, 1704351.

22 K. Radhakrishna, S. B. Manjunath, D. Devadiga, R. Chetri and A. T. Nagaraja, *ACS Appl. Energy Mater.*, 2023, **6**, 3635–3664.

23 J. Xia, P. Luizys, M. Daskeviciene, C. Xiao, K. Kantminiene, V. Jankauskas, K. Rakstys, G. Kreiza, X. Gao, H. Kanda, K. G. Brooks, I. R. Alwani, Q. U. Ain, J. Zou, G. Shao, R. Hu, Z. Qiu, A. Slonopas, A. M. Asiri, Y. Zhang, P. J. Dyson, V. Getautis and M. K. Nazeeruddin, *Adv. Mater.*, 2023, **35**, 2300720.

24 A. Farokhi, H. Shahroosvand, G. D. Monache, M. Pilkington and M. K. Nazeeruddin, *Chem. Soc. Rev.*, 2022, **51**, 5974–6064.

25 D. Li, J.-Y. Shao, Y. Li, Y. Li, L.-Y. Deng, Y.-W. Zhong and Q. Meng, *Chem. Commun.*, 2018, **54**, 1651–1654.

26 X. Zhang, X. Liu, F. F. Tirani, B. Ding, J. Chen, G. Rahim, M. Han, K. Zhang, Y. Zhou, H. Quan, B. Li, W. Du, K. G. Brooks, S. Dai, Z. Fei, A. M. Asiri, P. J. Dyson, M. K. Nazeeruddin and Y. Ding, *Angew. Chem., Int. Ed.*, 2024, **63**, e202320152.

27 M. SasiKumar, G. Maddala, M. Ambapuram, M. Subburu, J. R. Vaidya, S. N. Babu, P. Chetti, R. Mitty and S. Pola, *Sustainable Energy Fuels*, 2020, **4**, 4754–4767.

28 K. Manda, V. D. Jadhav, P. Chetti, R. Gundla and S. Pola, *Org. Electron.*, 2025, **136**, 107153.

29 G. Maddala, R. Gade, J. Ahemed, S. Kalvapalli, N. B. Simhachalam, P. Chetti, S. Pola and R. Mitty, *Sol. Energy*, 2021, **226**, 501–512.

This journal is © The Royal Society of Chemistry 2025

J. Mater. Chem. C, 2025, **13**, 13502–13508 | **13507**

30 D. Bharath, M. Sasikumar, N. R. Chereddy, J. R. Vaidya and S. Pola, *Sol. Energy*, 2018, **174**, 130–138.

31 A. Zhang, Y. Chen, Y. Xu, H. Wang, X. Zong, Z. Sun, M. Liang and S. Xue, *ACS Appl. Energy Mater.*, 2024, **7**, 11741–11753.

32 G. Zhang, F. R. Lin, F. Qi, T. Heumüller, A. Distler, H.-J. Egelhaaf, N. Li, P. C. Y. Chow, C. J. Brabec, A. K.-Y. Jen and H.-L. Yip, *Chem. Rev.*, 2022, **122**, 14180–14274.

33 Y. Liu, Q. Chen, H.-S. Duan, H. Zhou, Y. Michael Yang, H. Chen, S. Luo, T.-B. Song, L. Dou, Z. Hong and Y. Yang, *J. Mater. Chem. A*, 2015, **3**, 11940–11947.

34 C. Steck, M. Franckevičius, S. M. Zakeeruddin, A. Mishra, P. Bäuerle and M. Grätzel, *J. Mater. Chem. A*, 2015, **3**, 17738–17746.

35 E. Sheibani, L. Yang and J. Zhang, *Solar RRL*, 2020, **4**, 2000461.

36 H. D. Pham, S. M. Jain, M. Li, Z. Wang, S. Manzhos, K. Feron, S. Pitchaimuthu, Z. Liu, N. Motta, J. R. Durrant and P. Sonar, *Adv. Electron. Mater.*, 2020, **6**, 1900884.

37 A. Fülöpová, P. Magdolen, M. Károlyiová, I. Sigmundová and P. Zahradník, *J. Heterocycl. Chem.*, 2013, **50**, 563–567.

38 T. Malinauskas, D. Tomkute-Luksiene, R. Sens, M. Daskeviciene, R. Send, H. Wonneberger, V. Jankauskas, I. Bruder and V. Getautis, *ACS Appl. Mater. Interfaces*, 2015, **7**, 11107–11116.

39 S. Tian, X. Gao, D. Reyes, O. A. Syzgantseva, M. M. Baytemirov, N. Shibayama, H. Kanda, P. A. Schouwink, Z. Fei, L. Zhong, F. F. Tiranito, Y. Fang, P. J. Dyson and M. K. Nazeeruddin, *Small*, 2024, **20**, 2406929.

40 A. Jegorovė, J. Xia, M. Steponaitis, M. Daskeviciene, V. Jankauskas, A. Gruodis, E. Kamarauskas, T. Malinauskas, K. Rakstys, K. A. Alamry, V. Getautis and M. K. Nazeeruddin, *Chem. Mater.*, 2023, **35**, 5914–5923.

13508 | *J. Mater. Chem. C*, 2025, **13**, 13502–13508

This journal is © The Royal Society of Chemistry 2025